Fully 3-D-Printed Frequency-Scanning Slotted Waveguide Array With Wideband Power-Divider

Kunchen Zhao, Jordan A. Ramsey, and Nima Ghalichechian, *Senior Member, IEEE*

***Abstract*—We report the design, fabrication, and measurement results of a fully three-dimensional (3-D) printed frequency-scanning slotted waveguide array (SWA). The antenna system is composed of an 18 × 4 nonresonant (traveling wave) array operating at 12–18 GHz (Ku-band), a wideband 1 × 4 power divider, and four 50 Ω matched loads all fabricated using a 3-D printer and wet metallization steps. The antenna system is designed to be impedance-matched with S_{11} less than −10 dB across the entire band. Inductive walls are added to the power divider to improve the impedance matching of closely packed waveguides. Complex yet smooth waveguides are fabricated using the PolyJet technology. Conformal in-house metallization processes consisting of nickel electroless plating and copper electroplating are established. Measurement results show beam-scanning ranges from ±7° at 12 GHz to ±15° at 18 GHz. The maximum measured gain is 21.4 dBi with sidelobe level of −13.4 dB at 15.8 GHz and scanning angle of 7°. Furthermore, the array maintains minimum gain of 10 dBi for most of the band ranging from 13.4 to 17.8 GHz. Our measurement results are in an agreement with the simulations. This letter demonstrates a scanning array, together with a wideband power divider, and termination loads all fabricated using a 3-D printing technology.**

***Index Terms*—Frequency scanning, slotted waveguide array (SWA), three-dimensional (3-D) printed, wideband power divider.**

I. Introduction

BEAM steering is widely used in communication, radar, sensing, and navigation. One common approach is to use electronically scanned arrays or phased array antennas. While the phased array architecture has a superior performance, it is expensive and complex as it requires numerous phase shifters and transceivers [1]. Alternatively, for certain noncommunication applications, a frequency-scanning array can be used. In particular, a slotted waveguide array (SWA) exhibits low profile, high power handling, simple feed network, and mechanical robustness, making it a preferable candidate for space, airborne, and naval antennas. Traditionally, the SWAs are fabricated from brazed, machined plates and sheets or via electrical discharge machining [2]. These fabrication methods are usually time-consuming and expensive. Recently, advancements in additive manufacturing (AM) techniques have provided us with alternative avenues for the rapid fabrication of complex waveguide structures. To our knowledge, all the prior work in this area has concentrated on nonscanning arrays. For example, resonant SWAs at the millimeter-wave band were fabricated using three-dimensional (3-D) printing and reported to possess equivalent electromagnetic (EM) performance compared with metal antenna [3]–[5]. Although the resonant SWA fabrication using AM is now a mature technology, unique challenges (e.g., wideband feed structure) continue to hinder two-dimensional (2-D) nonresonant SWA.

Nonresonant SWA systems consist of three components: a wideband feed structure (usually waveguide power divider) [6], a traveling-wave array, and a matched load. One example of a one-dimensional (1-D) nonresonant SWA (without 3-D printing technique) was reported to operate at 130–180 GHz and was fabricated using a PolyStrata multilayer microfabrication process [7]. However, this process is expensive and slow. In this letter, we evaluate 3-D printing techniques for the realization of a nonresonant SWA. One of the challenges of designing the 2-D nonresonant SWA is the development of a wideband feed structure. Historically, an end-feed structure with π junction is utilized in SWAs [8]. However, the highest reported bandwidth is only 10%. Furthermore, bottom-feed structures for resonant SWAs [9] as well as corporate-feed for waveguide arrays [3] have low bandwidth. The research has shown that a waveguide power divider could have a wideband performance (above 40% fractional bandwidth) with high return loss in the millimeter-wave band [10]. However, since the physical structure of a waveguide array requires all output ports to be adjacent to each other, a traditional power divider cannot be directly connected to the SWA antenna. The use of inductive walls has been reported to improve the impedance matching of the power divider at a single frequency [11]. Other design challenges include symmetrical gain versus frequency pattern, termination, reduction of sidelobe, and location of nonradiating slots. Fabrication challenges include surface roughness (causing losses), conformal, and continuous metallization of waveguide inner surfaces using electroless and electroplating processes. As such, the main novelty of this letter is demonstration of a wideband scanning array with integrated wideband power divider and matched load using a 3-D printing technology.

II. Design

The architecture of the antenna system is shown in Fig. 1. Based on our prior work, we first constructed and simulated a 1-D SWA consisting of 18 slots [12], [13]. We then combined four identical 1-D units in parallel to form the 18×4 2-D array (72 elements). Nonradiating slots are added to aid the metallization process. The four-way power divider is designed to feed the array. Terminations of 50 Ω were carefully designed and

Manuscript received August 26, 2019; revised October 11, 2019; accepted October 29, 2019. Date of publication November 4, 2019; date of current version December 19, 2019. This work was supported in part by the U.S. National Science Foundation under Award #1711102. *(Corresponding author: Nima Ghalichechian.)*

The authors are with the Department of Electrical and Computer Engineering, The Ohio State University, Columbus, OH 43212 USA (e-mail: zhao.2889@osu.edu; ramsey.461@osu.edu; ghalichechian.1@osu.edu).

Digital Object Identifier 10.1109/LAWP.2019.2951324

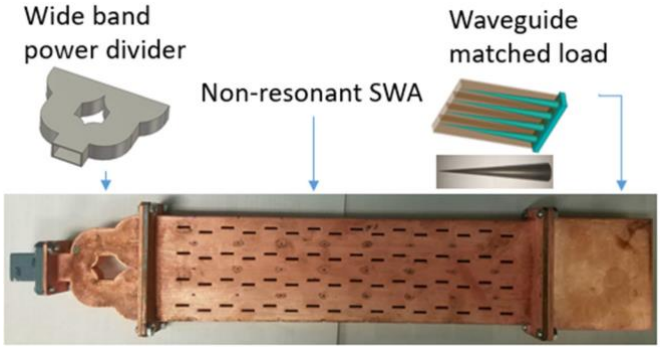

Fig. 1. Fabricated nonresonant SWA antenna system.

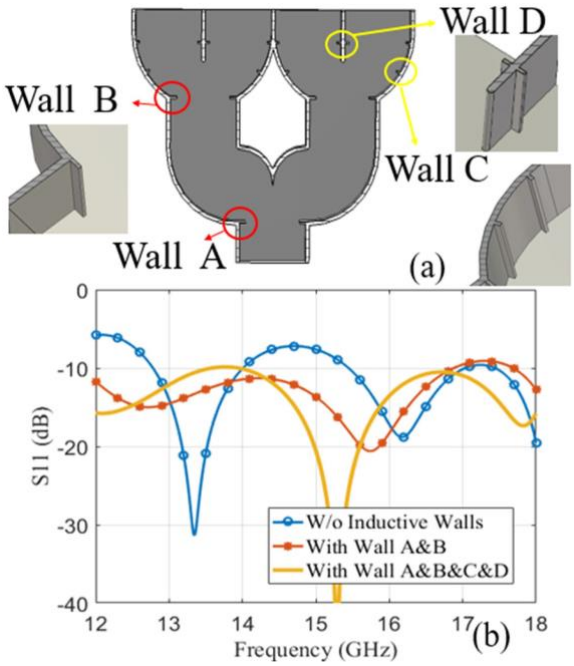

Fig. 2. (a) Four-way divider with inductive walls. (b) S_{11} of the four-way divider.

fabricated. Standard WR-62 waveguide size was used for all three aforementioned sections.

A. Wideband Power Divider

An end-feed structure is required to excite the SWA antenna. Small spacing between the adjacent elements (0.39 λ_0 at 15 GHz) makes the divider design extremely challenging. A four-way splitter is designed by cascading two two-way dividers. The wall thickness separating the two waveguides is 0.8 mm. The arc wedges are used to reduce the reflection due to the electromagnetic discontinuity. The design is simulated using time-domain solver in CST Microwave Studio. In the first design, each stage of the two-way power dividers achieved -10 dB. However, after cascading them to form a four-way divider, the S_{11} is added in phase to become -6 dB. Inductive walls are then added to the T-junction to improve the impedance matching. As shown in Fig. 2(a), the first group of inductive walls is added (marked as *A* and *B*). The simulated S_{11} is lower than -10 dB for 12–17 GHz after the first design iteration, showing

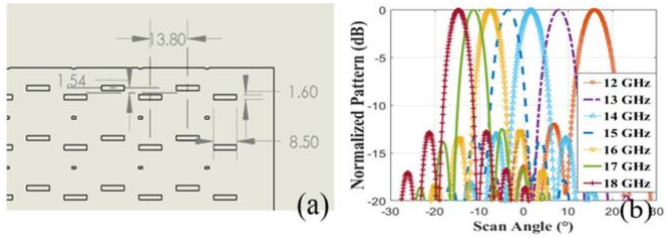

Fig. 3. (a) Critical SWA dimensions (units in mm). (b) Simulated *H*-plane realized gain from 12 to 18 GHz showing scanning range from 16.7° to +14.4°.

Fig. 4. 3-D model of the designed (a) front side and (b) back of the SWA without matched load and power divider.

significant improvement. However, as shown in Fig. 2(b), the S_{11} is still larger than $+0$ dB at 17–18 GHz. Therefore, the second group of the inductive walls is added to the arc wedges of the divider [marked as *C* and *D* in Fig. 2(a)]. Hence, the design includes 18 inductive walls, each with a thickness of 0.4 mm and the length varying between 1.0–1.6 mm. The overall length of the divider is 6.72 × 5.54 cm. Following this improvement, the S_{11} was lower than -10 dB for the entire Ku-band.

B. SWA Antenna

The SWA design follows the traditional scheme for traveling-wave antennas given by Eillott [14], [15], the detailed geometry of which is shown in Fig. 3. In order to demonstrate a 3-D scanning array, our design goal was to achieve a symmetrical beam scan range off the broadside as well as to maximize the gain symmetry. Alternatively, a flat-gain profile can be considered in similar designs. The scanning range correlates to the slot spacing, which is chosen to be 0.5 λ_0 at 14.2 GHz [shown in Fig. 3(a)]. The result is $-16.7°$ to $+14.4°$ *H*-plane scan range across the Ku-band as shown in Fig. 3(b). The slot spacing could be further increased to achieve a better symmetry of the beam scan range; however, the grating lobe will appear at higher frequency. The slot length determines the resonant frequency, which is optimized such that the gains at 12 and 18 GHz are the same. In other words, we have chosen a simple uniform design that has symmetric gain pattern off the broadside. In order to achieve constant sidelobe level (SLL) and half-power beamwidth (HPBW) performance over the entire frequency band, uniform slot distribution is chosen in the proposed antenna. The 3-D model of the designed array without the added loads and the power divider is shown in Fig. 4. The full-wave model (adapter, array, and termination) is fairly large and is composed of 79.9 million hexahedral mesh elements simulated using the CST time-domain solver.

In order to enhance the electroless and electroplating processes, nonradiating slots are added to provide access to the inside of the waveguide. The distance between slots of each

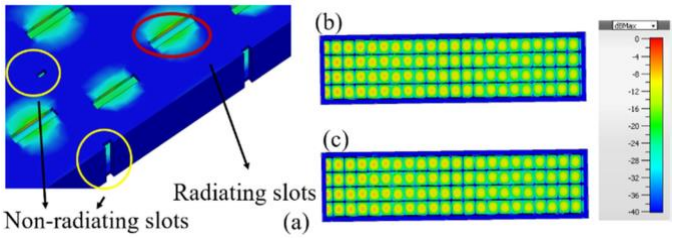

Fig. 5. (a) Surface *E*-field on radiating and nonradiating slots. (b) *E*-field inside the waveguide with and (c) without nonradiating slots (all at 15 GHz).

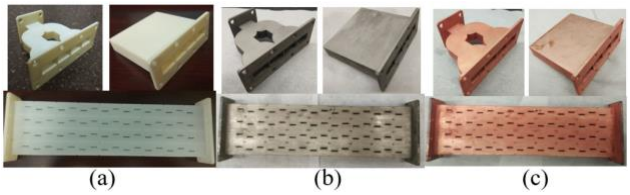

Fig. 6. Fabricated power divider, termination fixture, and waveguide array showing (a) 3-D-printed parts before metallization, (b) after Ni electroless plating, and (c) after Cu electroplating.

waveguide column is 16.6 mm. This is due to the size of WR-62 waveguide and the wall thickness of 0.8 mm. As shown in Fig. 5(a), the nonradiating slots are located on the narrow wall of the waveguide where the *E*-field and transverse surface current are zero. The location and size of the openings are both optimized by full-wave simulation. As shown in the Fig. 5(b) and (c), the *E*-field inside the waveguide remains the same before and after the addition of the nonradiating slots. Since the nonresonant SWA is a traveling-wave antenna, a matched load is required on the nonfeed end of the waveguide. Initially, we used 3-D-printed cones using lossy acrylonitrile butadiene styrene (ABS) material; however, only S_{11} >−15 dB was achieved due to low permittivity and loss. To improve the results, four commercially available WR-62 waveguide matched loads (CTL-0733, Resin System Corp., Amherst, NH, USA) with maximum ~~40~~ dB S_{11} were placed inside a third 3-D-printed waveguide fixture. The S_{11} of the commercial loads were independently measured to be less than −30 dB.

III. Fabrication and Measurement

A. PolyJet 3-D Printing

All three parts of the proposed SWA antenna (divider, radiating array, and termination) are printed using the commercial PolyJet process (Object 30 Prime from Stratasys) with VerowhitePlus photopolymer material. The fabricated parts are shown in Fig. 6(a). A PolyJet 3-D printing technique is chosen mainly due to its low surface roughness, strong adhesion, and smooth finish around edges.

B. Metallization

The metallization of the SWA system is performed in two consecutive steps: 1) the electroless plating of thin nickel (Ni) seed layer followed by 2) the electroplating of thick copper (Cu) film. These two processes, both developed in house, consist of several substeps. The Ni electroless plating consists of four substeps: etching, activating, fixing, and deposition. Following the first three initial steps, the parts are immersed in the electroless Ni plating solution, which is composed of a mixture of citric acid monohydrate, ammonium hydroxide, hydrochloric acid, Ni sulfate, and sodium hypophosphite. Ni plating is performed at a temperature of 41°C for 15 min. The 3-D-printed waveguides following the Ni plating have a smooth surface as shown in Fig. 6(b). After Ni plating, Cu is electroplated on each part [see Fig. 6(c)].

The electroplating is performed using copper-based electrolytic (Technic Inc., Cranston, RI, USA) intended for thick deposits. Under appropriate conditions, this solution can deposit high-purity fine-grain films. The solution is electrolyzed prior to use. The electroplating is performed at 30 °C for 30 min with current density of 0.05–0.15 mA/mm^2. The sheet resistance was measured using four-point probe and found to be 0.05 Ω/sq.

The slot length was measured to be 8.4 mm as compared to the designed value of 8.5 mm. The entire fabrication process can be completed in less than 48 h facilitating the rapid prototyping of the complex scanning array.

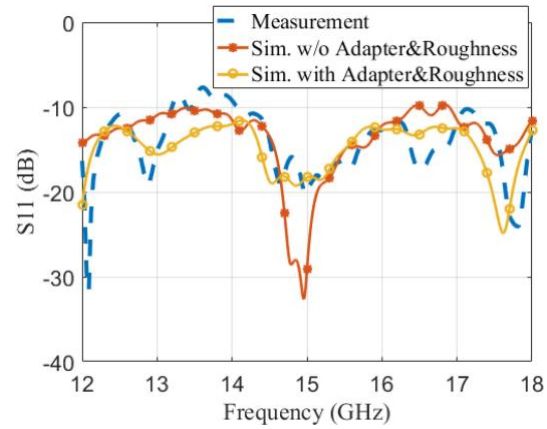

Fig. 7. Comparison of measured and simulated S_{11} of the SWA antenna including divider, antenna, and termination.

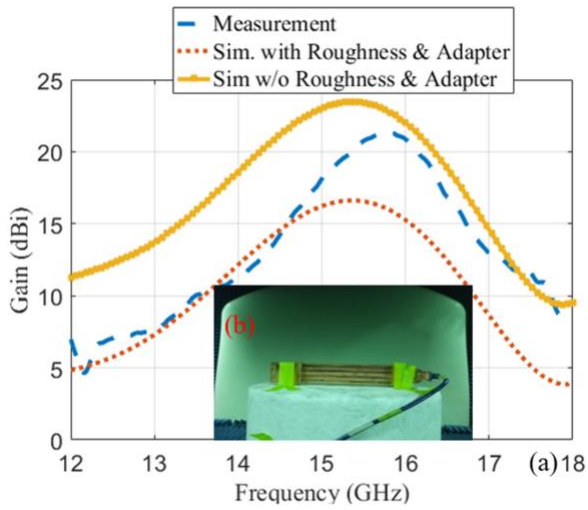

Fig. 8. (a) Comparison of measured and simulated gain at the boresight at Ku-band. (b) Pattern measurement setup in the anechoic chamber (slot length is 8.4 mm).

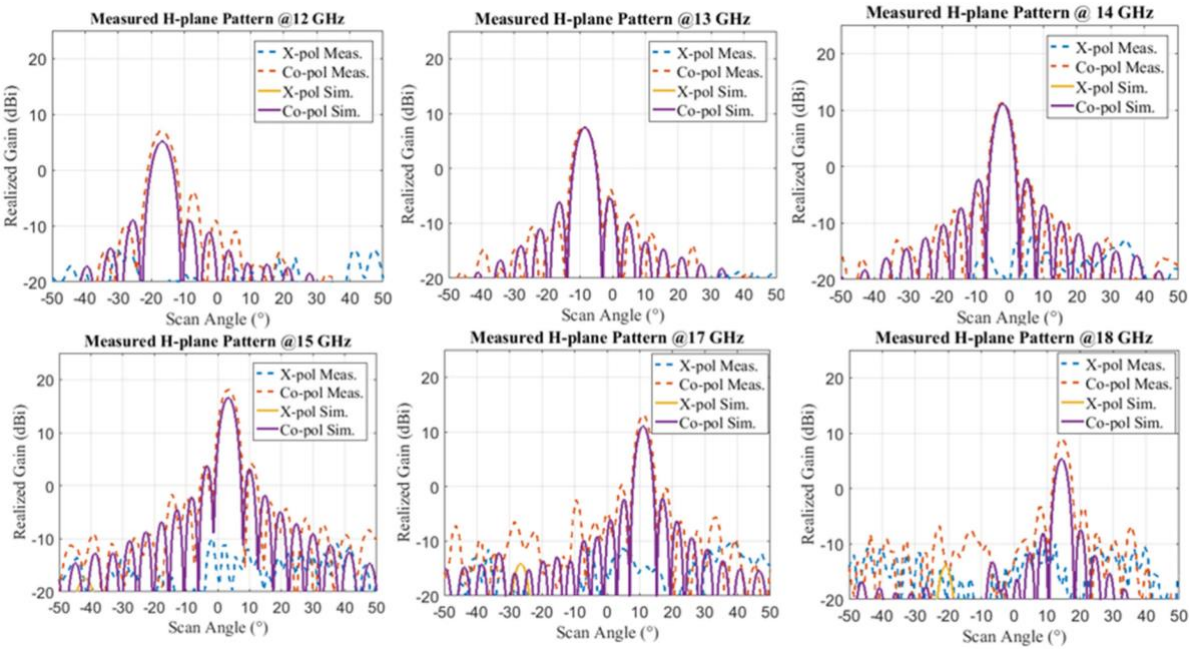

Fig. 9. Measured and simulated *H*-plane pattern from 12 to 18 GHz showing scanning range from −17° to +15°.

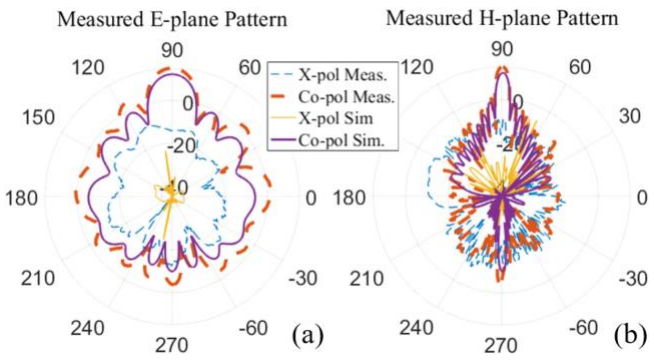

Fig. 10. Measured and simulated copol and cross-pol gains at 14.6 GHz (broadside) for (a) *E*-plane and (b) *H*-plane.

C. Measurement Results and Analysis

Prior to gain measurements, several 1-port and 2-port evaluations are conducted (Agilent N5230A PNA). Two identical power dividers are connected back-to-back. The measured S_{11} and S_{21} (not shown here) exhibit a good agreement with the simulation results. A 1-port measurement is performed on the final assembled SWA system including termination and power divider. The measured S_{11} and simulation results are shown in Fig. 7. The measured S_{11} matches well with the simulation results after adding the adapter and surface roughness. The average surface roughness is 17.8 μm root mean square measured by a contact profilometer and evaluated using the cannonball [16] model in our simulation. The modified simulation result indicates that the S_{11} is decreased by approximately 2 dB due to the conductive losses induced by the surface roughness. The adapter also induces nonideal behavior at the edges of the band, i.e., 12 and 18 GHz.

The radiation pattern is measured in the anechoic chamber [see Fig. 8(b)]. A 2–18 GHz standard horn antenna (H-1498) is used for calibration. Fig. 8 shows the measured gain of the boresight from 12 to 18 GHz. The maximum measured gain is 21.4 dBi at 15.8 GHz, while the maximum simulated gain is 18.6 dBi at 15.6 GHz (after applying the surface roughness). The maximum realized gain is decreased by 0–5 dB across the Ku-band due to adapter and roughness.

Fig. 9 shows the measured *H*-plane pattern ranging from 12 to 18 GHz as well as the simulation results. The measured scanning range is from −17.0° to +15.0°, showing a good agreement with the simulation results. The measured cross-pol is 20 dB less than copol at the boresight for all frequencies. Overall, the measured gain matches well with the simulation results. However, a minor discrepancy exists at 18 GHz possibly due to the fabrication error in a slot size and a rounding of the corners inside slots. Fig. 10 shows the measured and simulated polar pattern at 14.6 GHz (broadside). The measured SLL and HPBW for the *E*- and *H*-planes are −11.1 dB, 16.0° and −13.2 dB, 4.4°, respectively. The *E*-plane HPBW is reduced by 68° compared to a 1-D SWA. No strong back lobe is observed for either *E*- or *H*-plane. We note that irregular longitude slot spacing, due to fabrication imperfections, results in asymmetrical SLL.

IV. Conclusion

In this letter, we reported, for the first time, a 2-D Ku-band frequency-scanning SWA antenna using the 3-D printing technology. While nonscanning arrays have been previously reported, here we present a fully 3-D-printed scanning array with 72 elements operating at 12–18 GHz with unique features. These include a 3-D-printed low-loss wideband power divider, 50 Ω termination ports, two types of nonradiating slots, electroless plated nickel, and electroplated copper metallization layers inside the waveguide.

REFERENCES

[1] D. Parker and D. C. Zimmermann, "Phased arrays—Part I: Theory and architectures," *IEEE Trans. Microw. Theory Techn.*, vol. 50, no. 3, pp. 688–698, Mar. 2002.

[2] T. Anderson, H. Yun-Li, and J. Michalski, "Design and manufacturing techniques for planar slot array antennas for a variety of radar application," in *Proc. Int. Conf. IEEE Radar*, Dallas, TX, USA, 1998, pp. 337–342.

[3] G. Huang, S. Zhou, T. Chio, and T. Yeo, "Fabrication of a high-efficiency waveguide antenna array via direct metal laser sintering," *IEEE Antennas Wireless Propag. Lett.*, vol. 15, pp. 622–625, 2016.

[4] G. P. L. Sage, "3D printed waveguide slot array antennas," *IEEE Access*, vol. 4, pp. 1258–1265, 2016.

[5] J. Tak, A. Kantemur, Y. Sharma, and H. Xin, "A 3-D printed W-band slotted waveguide array antenna optimized using machine learning," *IEEE Antennas Wireless Propag. Lett.*, vol. 17, no. 11, pp. 2008–2012, Nov. 2018.

[6] S. V. H. René Camblor, M. Fernández, C. V. Antuña, and F. Las-Heras, "Submillimeter wavelength 2-D frequency scanning antenna based on slotted waveguides fed through a phase shifting network," *IEEE Trans. Antennas Propag.*, vol. 65, no. 7, pp. 3501–3509, Jul. 2017.

[7] L. R. van *et al.*, "Micro-fabricated 130–180 GHz frequency scanning waveguide arrays," *IEEE Trans. Antennas Propag.*, vol. 60, no. 8, pp. 3647–3653, Aug. 2012.

[8] M. A. J. Hirokawa and N. Goto, "Waveguide pi-junction with an inductive post," in *Proc. Int. Symp. IEEE Antennas Propag. Soc.*, 1992, pp. 2130–2133.

[9] Y. Q. A. Guennou-Martin, E. Rius, L. Fourtinon, and C. Person, "Design and manufacturing of a 3-D conformal slotted waveguide antenna array in Ku-band based on direct metal laser sintering," in *Proc. Int. Conf. IEEE Antenna Meas. Appl.*, Oct. 2016, pp. 1–4.

[10] L. L. Jianxing Li, Ling Lu, Hongyu Shi, Huimin Huo, and A. Zhang, "Four-way waveguide power divider design for W-band applications," *Int. J. RF Microw. Comput. Aided Eng.*, vol. 28, no. 5, 2018, Art. no. e21242.

[11] P. N. *et al.*, "Design of slotted waveguide array antenna Fed by H-plane power divider," in *Proc. Int. Conf. ATMS*, 2014, pp. 1–5.

[12] K. Zhao, G. Senger, and N. Ghalichechian, "3D-printed frequency scanning slotted waveguide array with wide band power divider," in *Proc. USNC-URSI Nat. Radio Sci. Meet.*, Jan. 2019.

[13] K. Zhao, G. Senger, and N. Ghalichechian, "Fabrication and characterization of 3D-printed Ku-band frequency scanning slotted waveguide antenna array," in *Proc. Int. Symp. IEEE Antennas Propag. USNC-URSI Radio Sci. Meet.*, Atlanta, 2019, p. 1.

[14] R. S. Eillott, "The desigh of small slot arrays," *IEEE Trans. Antennas Propag.*, vol. AP-26, no. 2, pp. 214–219, Mar. 1978.

[15] R. S. Elliott, "On the design of traveling-wave-fed longitudinal shunt slot arrays," *IEEE Trans. Antennas Propag.*, vol. AP-27, no. 5, pp. 717–720, Sep. 1979.

[16] L. Simonovich, "Practical method for modeling conductor surface roughness using the cannonball stack principle," in *Proc. Int. Conf. Des.*, 2015, pp. 1–23.